energies

MDPI

Article

Submarine Landslides and their Distribution in the Gas Hydrate Area on the North Slope of the South China Sea

Xuemin Wu [1,2], Qianyong Liang [1,2,*], Yun Ma [3,*], Yaohong Shi [1], Zhen Xia [1], Lihua Liu [4] and Matthias Haeckel [5]

1 Guangzhou Marine Geological Survey, China Geological Survey, Guangzhou 510070, China; wxm9211@163.com (X.W.); yaohongshi@21cn.com (Y.S.); xia-zhen@163.com (Z.X.)
2 Gas Hydrate Engineering Technology Center, China Geological Survey, Guangzhou 510070, China
3 School of Civil and Architectural Engineering, Yangtze Normal University, Chongqing 408100, China
4 Guangzhou Institute of Energy Conversion, Chinese Academy of Sciences, Guangzhou 510640, China; liulh@ms.giec.ac.cn
5 Leibniz Institute of Marine Sciences (IFM-GEOMAR), 24103 Kiel, Germany; mhaeckel@ifm-geomar.de
* Correspondence: tomlqy@hydz.cn (Q.L.); mayun@yznu.cn (Y.M.)

Received: 4 November 2018; Accepted: 11 December 2018; Published: 13 December 2018

Abstract: Integrated investigations have revealed abundant resources of gas hydrates on the northern slope of the South China Sea (SCS). Regarding the gas hydrate research of northern SCS, the gas hydrate related environment problem such as seabed landslides were also concentrated on in those areas. Based on 2D seismic data and sub-bottom profiles of the gas hydrate areas, submarine landslides in the areas of Qiongdongnan, Xisha, Shenhu, and Dongsha have been identified, characterized, and interpreted, and the geophysical characteristics of the northern SCS region investigated comprehensively. The results show 6 major landslides in the gas hydrate zone of the northern SCS and 24 landslides in the Shenhu and Dongsha slope areas of the northern SCS. The landslide zones are located mainly at water depths of 200–3000 m, and they occur on the sides of valleys on the slope, on the flanks of volcanoes, and on the uplifted steep slopes above magmatic intrusions. All landslides extend laterally towards the NE or NEE and show a close relationship to the ancient coastline and the steep terrain of the seabed. We speculate that the distribution and development of submarine landslides in this area has a close relationship with the tectonic setting and sedimentary filling characteristics of the slopes where they are located. Seismic activity is the important factor controlling the submarine landslide in Dongsha area, but the important factor controlling the submarine landslides in Shenhu area is the decomposition of natural gas hydrates.

Keywords: submarine landslides; landslide types; distribution characteristics; gas hydrate; South China Sea

1. Introduction

Submarine landslides are a common geological phenomenon and also one of the most dangerous geohazards [1]. Landslides have led to many significant losses in the marine world and have attracted the attention of many [2–5], thus providing a motive for our study, but the problem is that it is not generally possible to monitor or directly observe submarine landslides due to their occurrence under the sea [3,6–11].

Natural gas hydrate (also called methane hydrate) is viewed as a potential new energy sources in the future. The bottom-simulating reflector (BSR) is a geophysical indirect marker of the presence of gas hydrates, caused by free gas underneath the hydrate layer [12]. The BSR is characterized by a high

reflection amplitude and negative polarity, and broadly parallel to the seafloor in seismic profiles [13]. Submarine landslides in the gas hydrate areas, has aroused people special concern on the environment effect. Although some progress have been made in determining the morphological characteristics, timing, frequency, and controlling factors of submarine landslides [1,14–17], there is little research on submarine geohazards that are closely related to gas hydrates [18–20], and further research on their evolutionary processes is necessary.

At present we know very little about the mechanism of submarine landslides in relation to gas hydrates, and several studies were done to reveal the relationship between submarine landslides and the gas hydrates bellow the seafloor. Magmatic sills may generate large amounts of methane releasing and storage beneath subsurface when geothermal gradients drop [21]. Somoza et al. (2018) report the relationships between sills and landslides in Antartica. They indicate that the diagenetic alteration of siliceous deposits is a possible cause of slope instability along high-latitude continental margins and oceanic basin. [22]. Gas hydrate studies on the northern Cascadia margin indicate possible link between slope failure and the presence of hydrates in the seafloor sediments [23]. Particularly, Yelisetti et al. (2014) indicate that the glide plane for slope failure is provided by contrast in sediments with and without hydrates [23,24]. One of the scientific targets of the IODP expedition 372 is to elucidate the creeping mechanism of landslides that contain gas hydrates at the edge of the Hikurangi subduction shelf of New Zealand using the methods of drilling and logging-while-drilling [11]. In recent decades, many conventional oil and gas reservoirs have been found on the continental margin of the northern part of the South China Sea (SCS). Huge reservoirs of natural gas hydrates were discovered in these areas [25–28]. Much of the previous research on the continental shelf and upper continental slope of this area has paid little attention to the hydrate-related geohazards in these areas [29–35]. Although research has been done on submarine landslides in areas of natural gas hydrate exploration [32–38], the focus has been mainly on the spatial distribution and geometric characteristics of the landslides. Unfortunately, the relationships between the distribution of gas hydrates and the characteristics of submarine landslides, such as their classification, geomorphic features, distribution, and genesis, have not been investigated systematically [36,39–42].

In 2017, great success was achieved by China Geological Survey on gas hydrate production test in Shenhu, SCS, and no environmental problems were occurred during the production [43,44]. In this study, we use 2D seismic data for the area of gas hydrate production on the northern continental slopes of the SCS to (1) show we also concern about the environment problem with regard to gas hydrate during exploitation and production; (2) analyze the relationships between submarine landslides in the area and the formation and dissolution of gas hydrates. Based on a comprehensive description and analysis of the seismic features, and the types, spatial distribution, and internal characteristics of the submarine landslides, some controls on the distribution of these submarine landslides are proposed, laying a foundation for further research. Our results provide a basis for further work on the hydrate mineralization effect, gas hydrate exploration, and disaster prevention and mitigation.

2. Geological Background

The study areas are located at the intersections of the Eurasian, Philippine, and SCS plates [45]. The north shelf of south China Sea includes four areas, which are Qiongdongnan area, Xisha area, Shenhu area, and Dongsha area (as shown in Figure 1). Most of our work has been focused on the Shenhu and Dongsha areas. The blue lines with numbers denote the 2D multichannel seismic section lines location. The seismic profiles were shown from Figures 2–11, processing by post-stack time migration. The tectonic and geological settings of the study areas, as well as their seabed topographic features, are unique and complex.

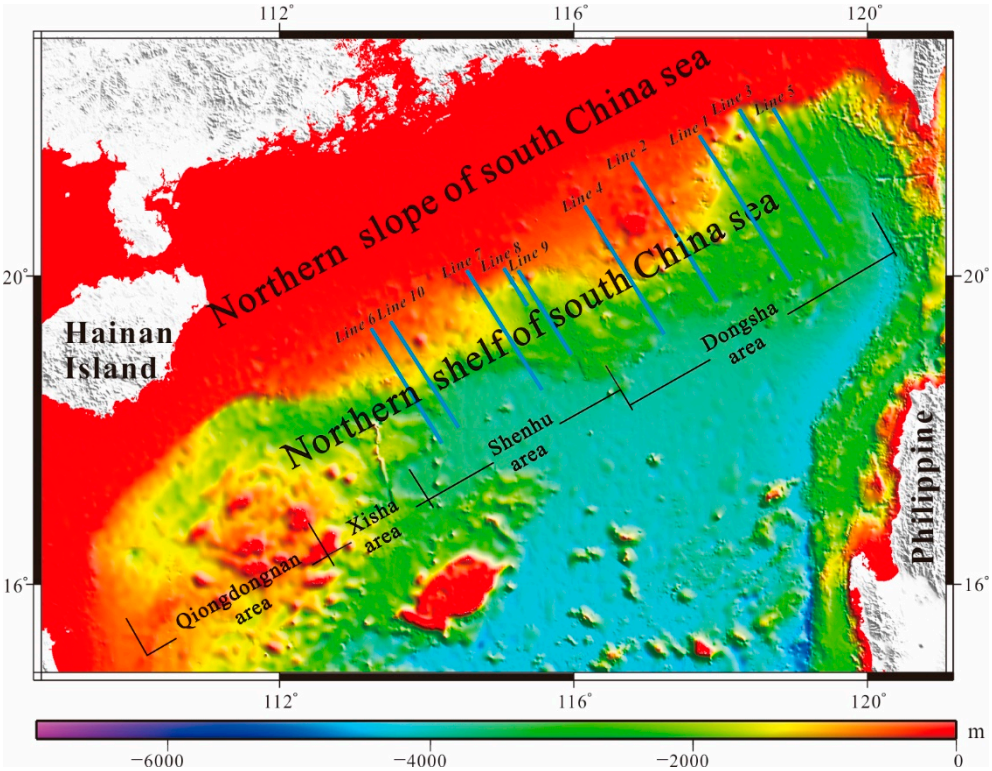

Figure 1. Location of study area-the northern slope of South China Sea [48].

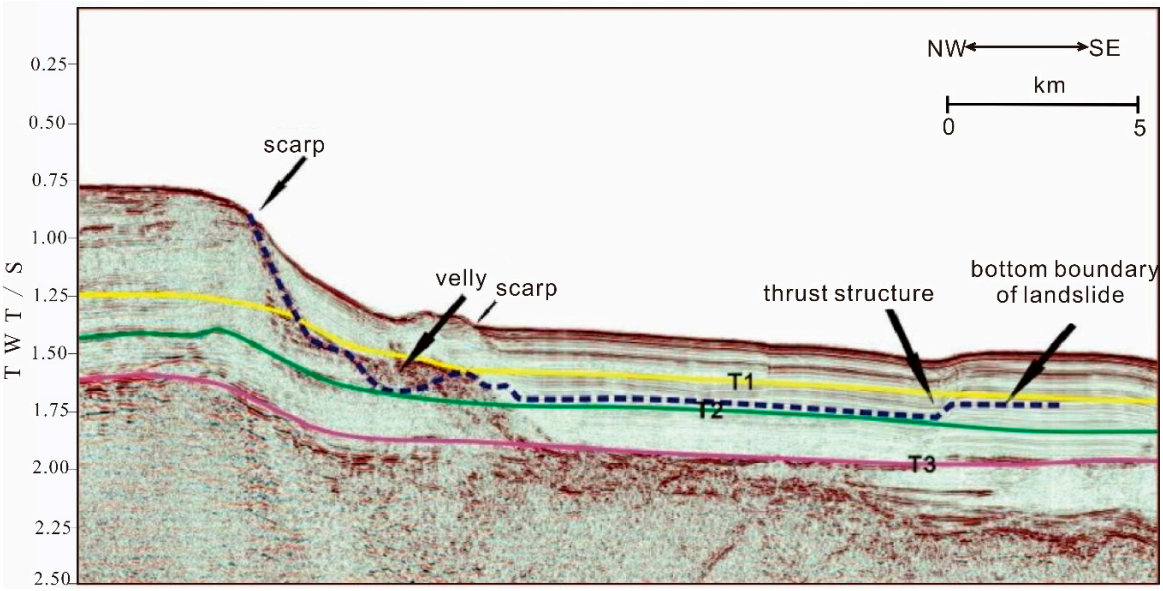

Figure 2. Seismic reflection of landslide of Line 1 on the northern slope of South China Sea.

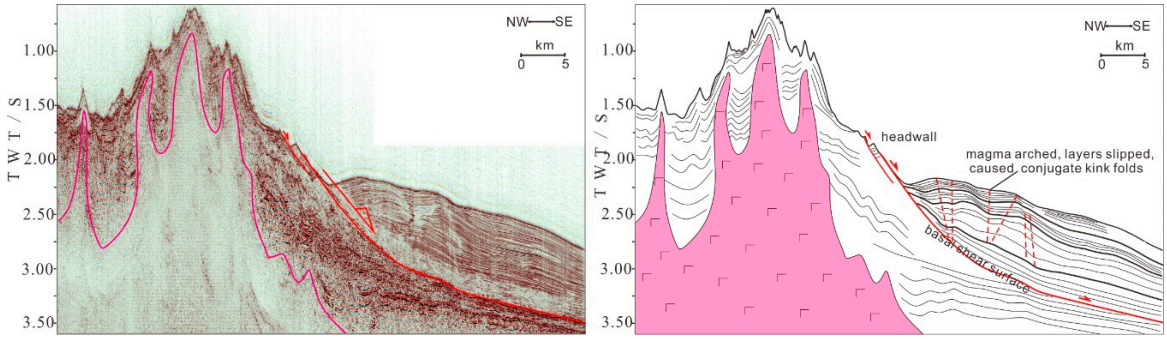

Figure 3. Seismic reflection profile of Line 2 is a landslide induced by piercing intrusive rocks and interpretation model.

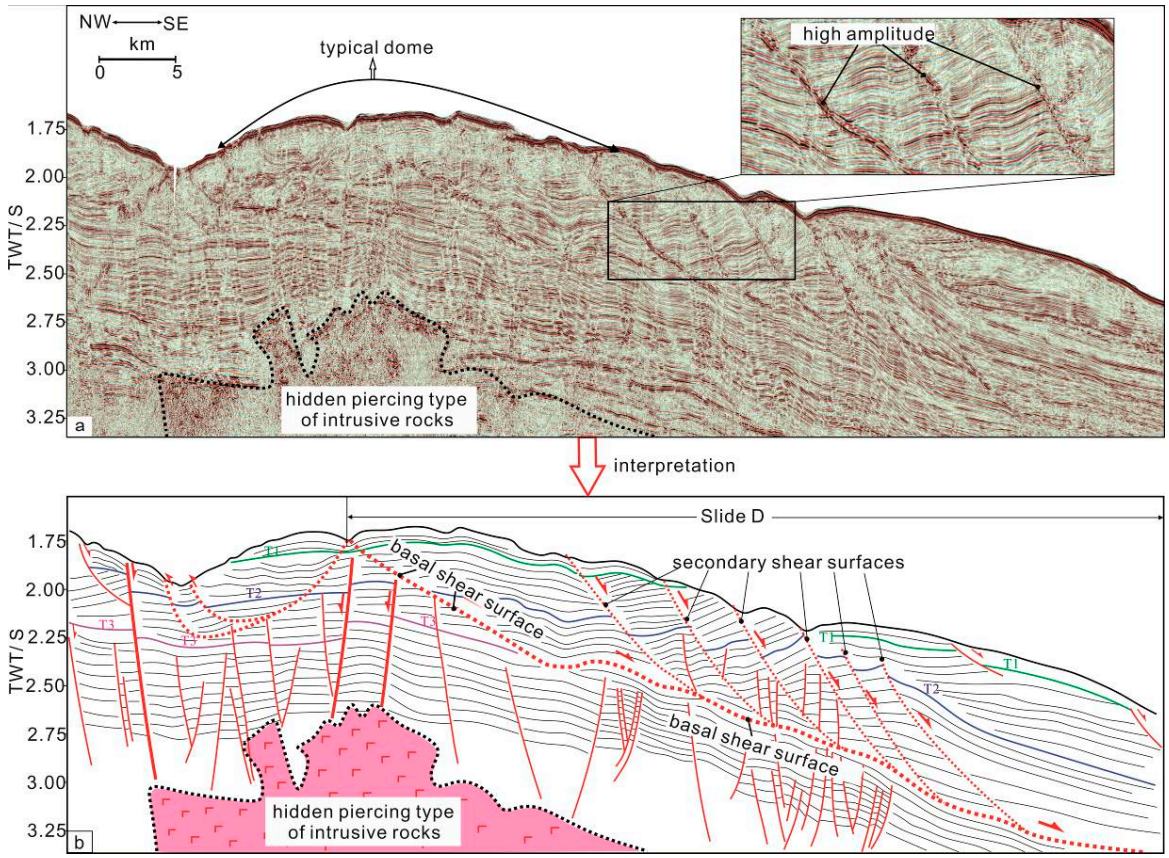

Figure 4. Seismic reflection profile of Line 3 is a landslide induced by hidden piercing intrusive rocks and interpretation of genetic model.

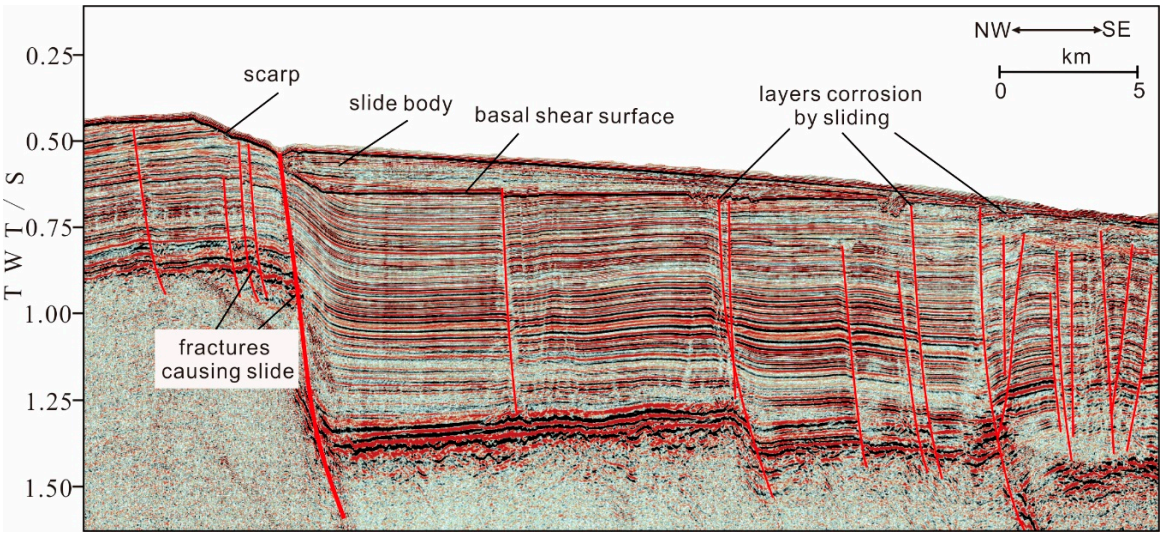

Figure 5. Seismic reflection of Line 4 is a landslide induced by fractures.

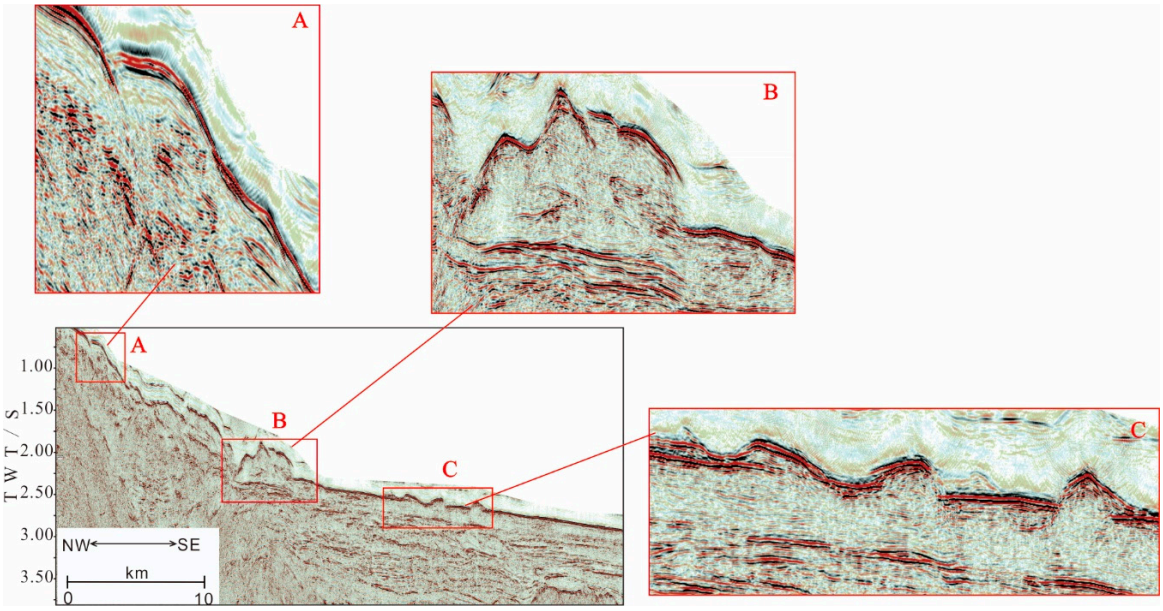

Figure 6. Seismic reflection of Line 5 is a landslide induced by earthquake.

The region has undergone multi-stage tectonic activities since the beginning of the Cenozoic, resulting in frequent magmatic activity in some areas and intensive fault activity [36]. A series of Cenozoic tectonic movements happened in the study areas, such as the Shenhu, the South China Sea, the Dongsha, as well as consequential erosion and deposition, thus resulting in the general development of a unique submarine sedimentary landscape that has given rise to the current geohazards on the northern slope of SCS [34].

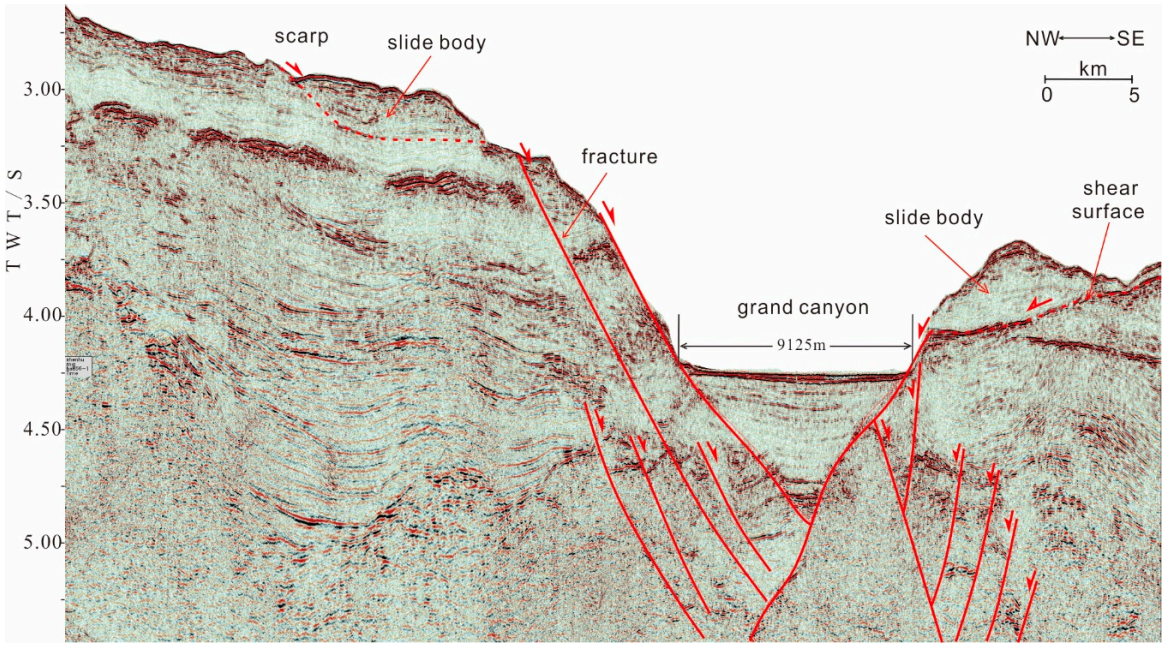

Figure 7. Seismic reflection of Line 6 is a landslide induced by erosion.

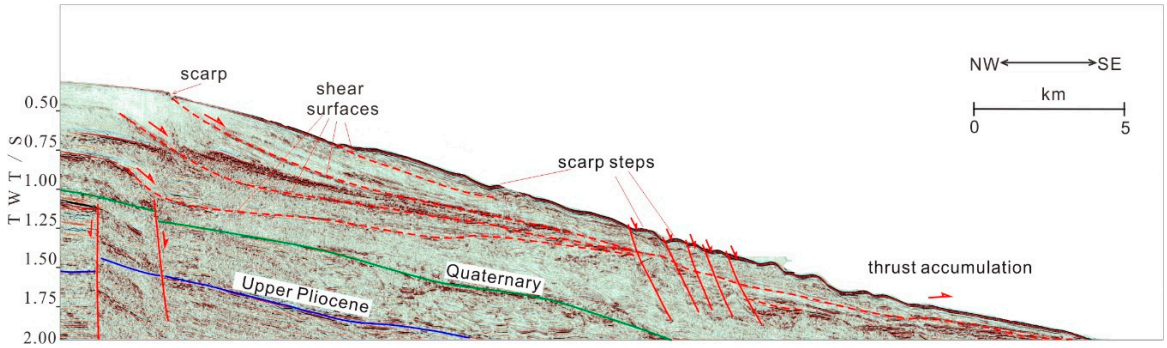

Figure 8. Seismic reflection of Line 7 is a landslide induced by slope breaking.

The gas hydrate deposition areas are at water depths of 200–3700 m. The first-order geomorphic type of the study area belongs to the category of continental slope. According to the classification of the SCS by Feng et al. [29], the continental slope is the area between the continental shelf and the boundary of the deep-sea plain, and it is more complex than these latter two regions [29]. Northeastwards from the outer edge of the continental margin of Qiongdongnan, and to the east of the island of Taiwan, the water depth increases gradually from 200 m to about 3400 m (as shown in Figure 1), and the topography is rugged and fluctuating with steps down towards the southeast. Tectonic activity in the northwest of the SCS area in the Cenozoic has been strong, with numerous NNE–SSW, NEE–SWW, and NWW–SEE faults having formed [46]. Moreover, Cenozoic deposition rates (>150 m/Ma) are generally high in this area, resulting in thick accumulations of fine-grained sediments [47]. It seems, that this unique tectonic setting and the abundant supply of sediment were the underlying causes of the anomalous development of submarine landslides in this area.

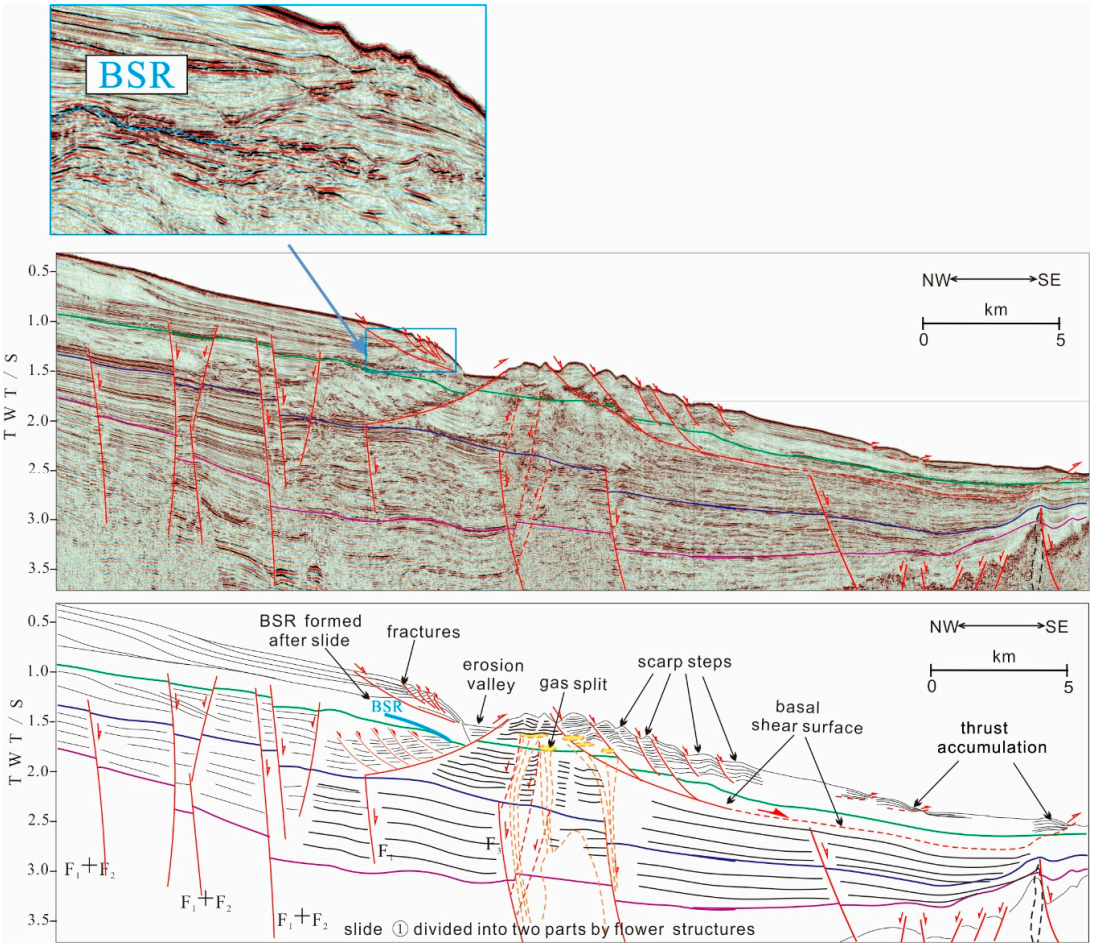

Figure 9. Seismic reflection of Line 8 is a pre-gas hydrate landslide with its interpretation.

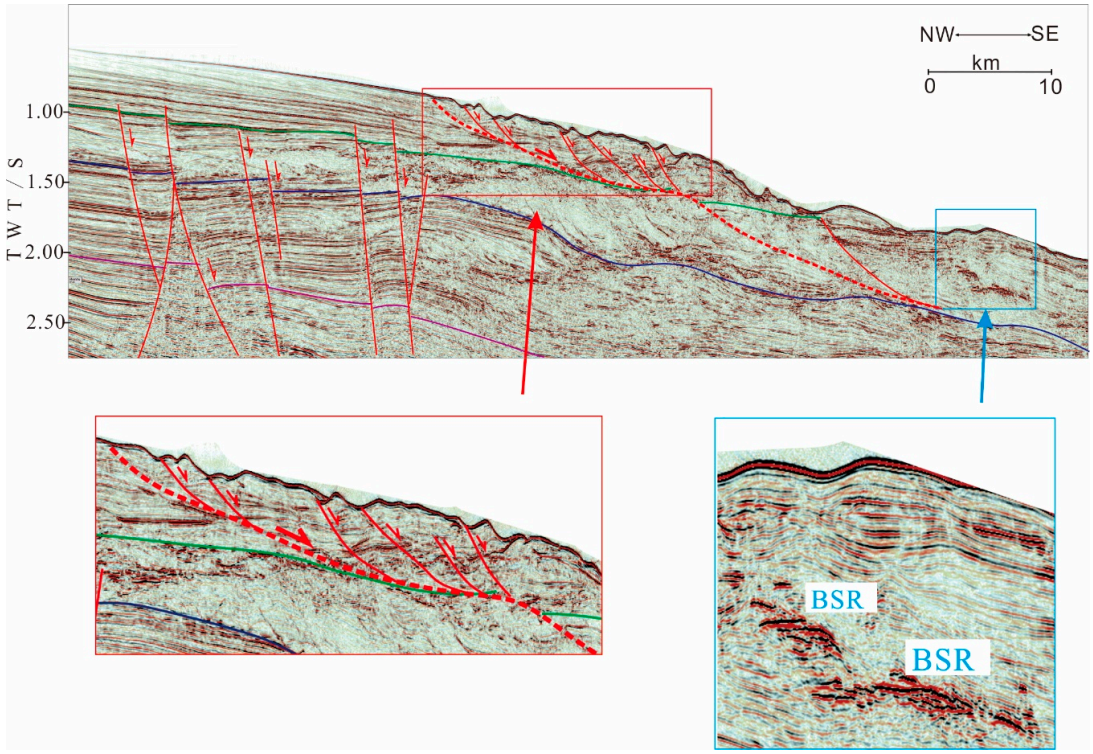

Figure 10. Seismic reflection of Line 9 is a landslide with hydrate located inside its body.

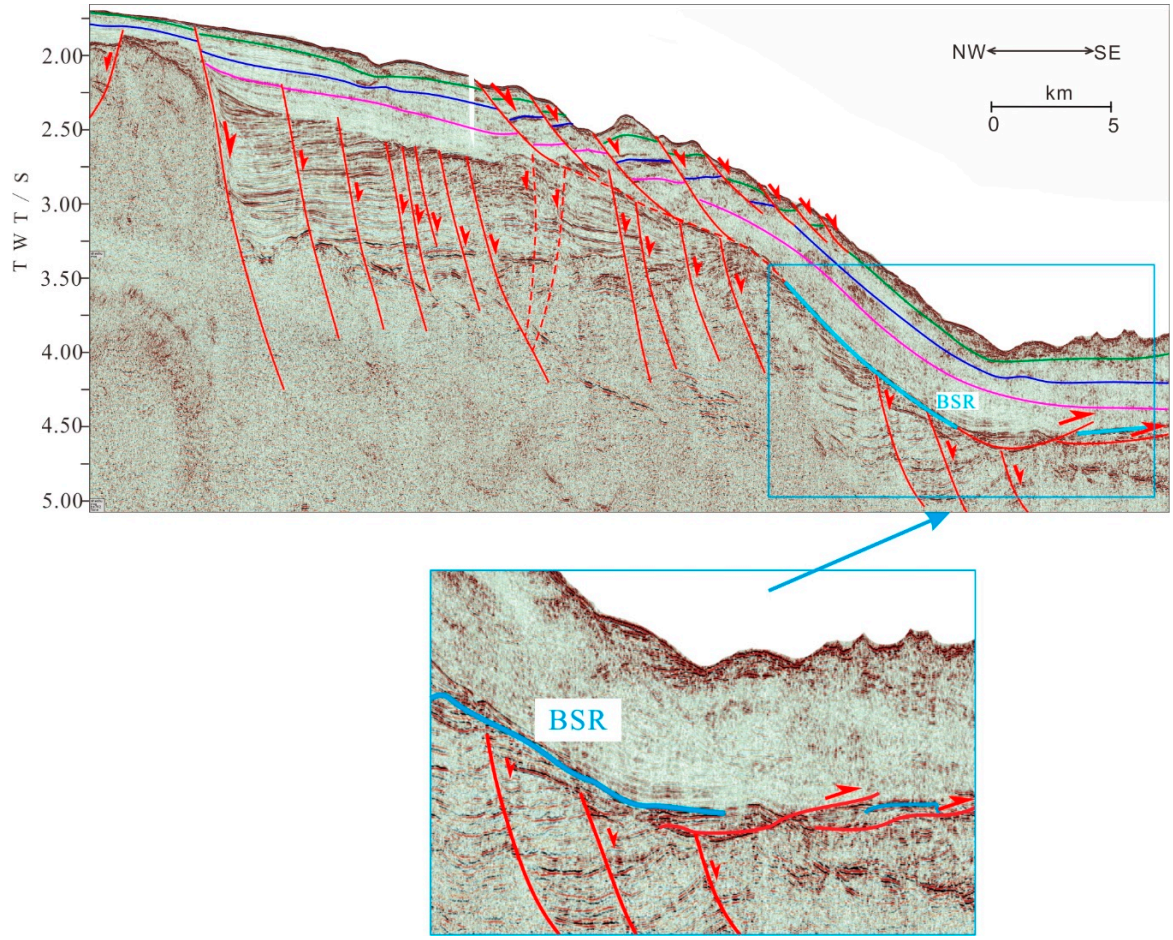

Figure 11. Seismic reflection of Line 10 is post-gas hydrate landslide.

3. Data Acquisition and Processing

The 2D multichannel seismic data of blue Line in Figure 1 were acquired by crews of TanBao vessel which comes from Guangzhou marine geological survey (GMGS). The main seismic survey equipment used during data acquisition include: ORCA integrated navigation and positioning system, BOLT air gun source system, BigShot air gun controller, SEAL seismic record system, and Focus5.0 seismic data processing system. The channel interval is 25 m, and the minimum offset is 175 m. The sample rate of acquisition is 2 ms. The low and high cut-off frequency are 4 Hz and 600 Hz respectively.

To get the high-quality seismic profiles (Figures 2–11), the original data were precisely processed by Omega2012 seismic processing system. The main processing flow includes: noise attenuation, amplitude compensation, deconvolution, velocity analysis, and post-stack time migration. After getting the high resolution and high signal to noise ratio (SNR) seismic data, these seismic profiles were interpreted by the Geoframe seismic interpretation system.

4. Types of Seabed Landslide and Their Developmental Characteristics

The relationships between landslide surfaces, formation boundaries, and the structures of the sliding body are clearly revealed in seismic profiles of the study areas. The location of Line 1 in Figure 2 is shown in Figure 1. The scarps (steep slopes), collapsed valleys (V-shaped valleys, U-shaped valleys, depressions, and eroded troughs), landslide mass (slidable slopes or slugs), landslide surface (landslide bottom), and landslide steps (multi-level landslide mass with a slightly tilted surface morphology) are revealed in profile (Figure 2). The scarp formed generally because of landslides. T1, T2, T3 are three target layers of this study area. The landslide boundary is almost parallel with

the target layer (Figure 2). The landslide surfaces are curved, and the occurrence of a landslide mass has the same direction as the landslide surface. Opposing slopes form raised steps at the top ends of the landslides, revealing the nature of the initial stage of landslide formation, so we can see the thrust structure in Figure 2. Landslide surfaces overlap and cross-cut each other, often with the strata rotated. In Figure 2, The lithology of the upper surface of a submarine landslide is a coarse or fine sand, whereas the lower basal part is a clayey sand. The increase in clay content towards the base, and the occasional development of clay interlayers, leads to high hydrophilicity, shrinkage, disintegration, and poor shear resistance. The apparent differences in lithology between the upper and lower landslide surfaces constitute an objective condition for sliding.

Recent landslides are distributed on the present seabed, often bury earlier landslides, and constitute a considerable hazard for any marine engineering. Feng et al. [29] provided the following scheme of classification for submarine landslides in our study area: they can be divided into super-large, large, medium, and small landslides according to their landslide sizes, thicknesses, structure of the sliding slope, location of the sliding surfaces, and other considerations; they can also be divided into thin layer, medium layer, thick layer, and very-thick layer types according to their thicknesses; and they can be divided into no-layer landslides, along-layer landslides, and cutting-layer landslides according to the structure of the slide slope and the location of the landslide surface. However, this classification does not take into account the mechanism of formation of the landslides or their relationships with gas hydrates, which makes the scheme difficult to apply in gas hydrate areas. To surmount this problem, we present six categories of submarine landslides in the Shenhu and Dongsha areas, including magmatism-related landslides, fault-related landslides, seismicity-related landslides, erosion-related landslides, slope-break landslides, and hydrate-related landslides.

4.1. Magmatism-Related Landslides

Magmatism-related landslides are caused by the rise of a magma diapir, or the puncturing of rocks by magma, which causes the strata to be thrusted or distorted, eventually leading to the formation of a slip and a landslide. These landslides can be further divided into magma-puncture landslides, and Magma-intrusion landslides, according to whether the magmatic material is exposed on the seabed or not.

A magma-puncture landslide is shown in Figure 3. The formation of magma-puncture landslides involves strong magmatic activity with the formation of a submarine volcano, so that the submarine strata around the volcano are pushed up, making them vulnerable to the formation of landslides (the pink area in Figure 3). This kind of landslide results from the tensile stresses associated with volcanic activity, and the strata in the landslide closer to the volcano show more intense folds, including conjugate kink folds (Figure 3). The folds weaken and gradually disappear away from the volcano in Figure 3. The red arrow denotes the slip direction of those folds.

A magma-intrusion landslide is shown in Figure 4. The formation of magma-intrusion landslides does not involve the cross-cutting of the sediments on the seabed by magma, but they involve the uplift and arching of surficial sediments due to the ascent of the underlying magma. Because of this uplift, the tilted strata eventually fail, and they slide under the influence of gravity parallel to the sedimentary layers. The landslides developed simultaneously on both sides of the uplifted zone (Figure 4). This landslide is characterized by being initiated at the high points of the uplifted area, and by their movement perpendicular to the axis of the arch. In Figure 4b, there are some secondary shear surfaces over the long continuous basal shear surface. Those secondary shear surfaces are characterized by the high amplitude in seismic section. These slides show a regular arrangement of strike slip surfaces along their edges, where they neatly cut the remaining strata, and the main slip surfaces are clearly visible.

4.2. Fault-Related Landslides

Fault-related landslides are caused by the tilting and fracturing of strata due to the reactivation of a fault or the tilting of a fault block. The landslides form with the strongly developed fracturing, and the magnitude of the fracturing determines the intensity of the landslide and the distance it travels (Figure 5). The length of slide body could be almost 20 km. The layers corrosion by sliding and the basal shear surface interpreted in Figure 5 denote an unconformity. A series of thrust structures is shown in Figure 5, which usually form during the progressive development of the landslide.

4.3. Seismicity-Related Landslides

Seismicity-related landslides are usually caused by strata instability triggered by seismic activity. Taking into account the seismic distribution map of the northern SCS [34], we compared the seabed landslides in areas where earthquakes are concentrated (northeast of the Dongsha area) with those in areas free of earthquakes, and we found obvious differences in their characteristics. one of the seismic profile in Dongsha area is shown in Figure 6. In this seismic reflection profiles, landslides in the areas where earthquakes are concentrated usually have the characteristics of landslide collapse (Figure 6A), and the slip surface may not be clear (Figure 6B). The landslides are broken up, and internal reflections of the landslide bodies are cluttered or blank (Figure 6C), and we assume that the shaking of the earthquake caused the destruction of the internal structure of the landslide. Therefore, we consider that the submarine landslides in the Dongsha gas hydrate area, where earthquakes are concentrated, are seismicity-related landslides. Besides, compare the profiles in Figure 6 and the profile in Figure 5, the earthquake-related landslides show more destructive in slip surface and landslide bodies could be more chaotic. we suggest that there are significant differences between seismicity-related landslides and fault-related landslides in seismic profile.

4.4. Erosion-Related Landslides

Erosion-related landslides are due mainly to the effects of water, where erosion has removed the strata to form valleys or troughs. In Figure 7, The length of grand canyon is 9125 m. Both sides of grand canyon have some fractures. With ongoing erosion, the gradient of the valley slope increases to gradually achieve the slope necessary to produce a landslide under the influence of gravity. If the valley slope is large enough, the landslide itself will be prone to collapse. This type of landslide is usually incomplete since the leading edge of the landslide often falls into the valley and is then completely or partially eroded. The interiors of such landslides are often fractured due to rapid sliding. Moreover, as erosion continues, further landslides may occur, and the early landslides may be caught up repeatedly in a succession of slides, and the range of the landslides will be extended gradually outwards. We assume that the slide body in Figure 7 would lead to the second landslides in the future, if the erosion had increased in the zone of grand canyon. Erosion-related landslides have been found in the seismic sections of the Shenshu and Dongsha areas, and these landslides have combined to form a belt of landslides on adjacent seismic sections (shown in Figure 7). We assumed a typical zone of erosion-related landslides is already well developed both in the Dongsha and Shenhu areas.

4.5. Slope-Break Landslides

Slope-break landslides are located mainly at the inflexion points where the slope breaks from that of the continental shelf to that of the continental slope, and where the natural angles of the slope-break lead to the sliding of sedimentary layers down the slope due to the forces of gravity to form submarine landslides. In Figure 8, typical slope-break landslides were initiated in the Shenhu slope-break area, and several shear surfaces are shown in the profile. At the bottom of these landslides, a multi-stage buried delta is usually developing (the scarp steps in Figure 8). The evidence of strike slip movements and thrusts in these slope-break landslides can be seen clearly in the seismic profiles as shown in Figure 8.

4.6. Hydrate-Related Landslides

Previous studies have shown that some submarine landslides are closely related to gas hydrates [46]. As a result of our research, we defined a special class of landslides called hydrate-related landslides, and we can further subdivide this class into three types: pre-, post-, and syn-hydrate landslides, based on the temporal relationship between the gas hydrate and the seabed landslide [49].

4.6.1. Pre-Hydrate Landslides

Pre-hydrate landslides developed before the formation of the gas hydrate deposits. In Figure 9, BSR formed along the slip surface, means that the gas hydrate has developed at the slip surface of the landslide, due to the plugging effect of the slip surface. This plugging effect is a result of the strong plasticity of these landslides, so that fissures formed by stretching are filled rapidly with fine-grained sediments. The overlap of tectonic and gravity force caused higher pressure of the fault plane, and the friction of the sliding surface increasing, which leads to the finer particles, denser structure, and lower permeability. In the other side of erosion valley, the plugging structure did not form when landslide happened, so we can see gas split, instead of the signal of BSR (Figure 9).

4.6.2. Syn-Hydrate Landslides

The syn-hydrate landslide is that the process of hydrate formation coincides with the occurrence of the landslide. In other words, the occurrence of the seabed landslide provides favorable conditions for gas hydrate formation. If such landslide becomes inactive, the gas hydrate deposits will be preserved, but they have the potential to be released in the future. Sometimes the hydrate is located inside the slab body, as shown in Figure 10. The signal of BSR in blue box is continuous. We assumed that the rapid accumulation of some landslides, which also provide a good gas source if the temperature and pressure conditions are appropriate. If such landslide is no longer active, the hydrates may be retained, but if landslide activity is rejuvenated, gas hydrate decomposition may ensue.

4.6.3. Post-Hydrate Landslides

Post-hydrate landslides develop on the seabed after formation of the gas hydrate deposits, and this type of landslide may be caused directly by the partial or complete decomposition of the gas hydrates. The post-hydrate landslide is shown in Figure 11, and the BSR is distributed along the sliding surface but not continuous. The fracture with red arrow in blue box developed after formation of gas hydrate deposits, and we assume the decomposition of the gas hydrates may cause the deterioration in strata stability. The strata instability would lead to the development of a series of slip faults, mainly at front of the residual hydrates. The vertical blank zone in Figure 11 is a data gap caused by the seismic muting process before the gather stack.

5. Spatial Distribution and Genesis of the Submarine Landslides

In our study area, the continental slope itself is an important factor in the development of seabed landslides, but several other factors also contributed to the production of topographical features that provided favorable conditions for seabed landslides, and these include the general tectonic activity in the area, the presence of volcanoes, the puncturing or uplift of the seabed as a result of magma movements, and differential uplift due to Neotectonic movements [34,37]. The geological, geomorphological, and geophysical data reveal 24 landslides in the Shenhu and Dongsha areas of the continental slope, and in Figure 12 we show how the various categories of these 24 landslides are distributed. The landslides are located mainly in water depths of 200–3000 m, and they are distributed mainly in the slope-break area, on both sides of volcanoes and valleys, and on the steep slopes of uplifted areas above magmatic intrusions. They generally extend laterally towards the NE or ENE, as shown in Figure 12, and their locations are closely related to ancient coastlines and the steep slope of the seabed terrain. It seems, therefore, that the distribution and development of these submarine

landslides were closely related to the tectonic and geological settings, as well as the nature of the sedimentary deposits on the continental slope.

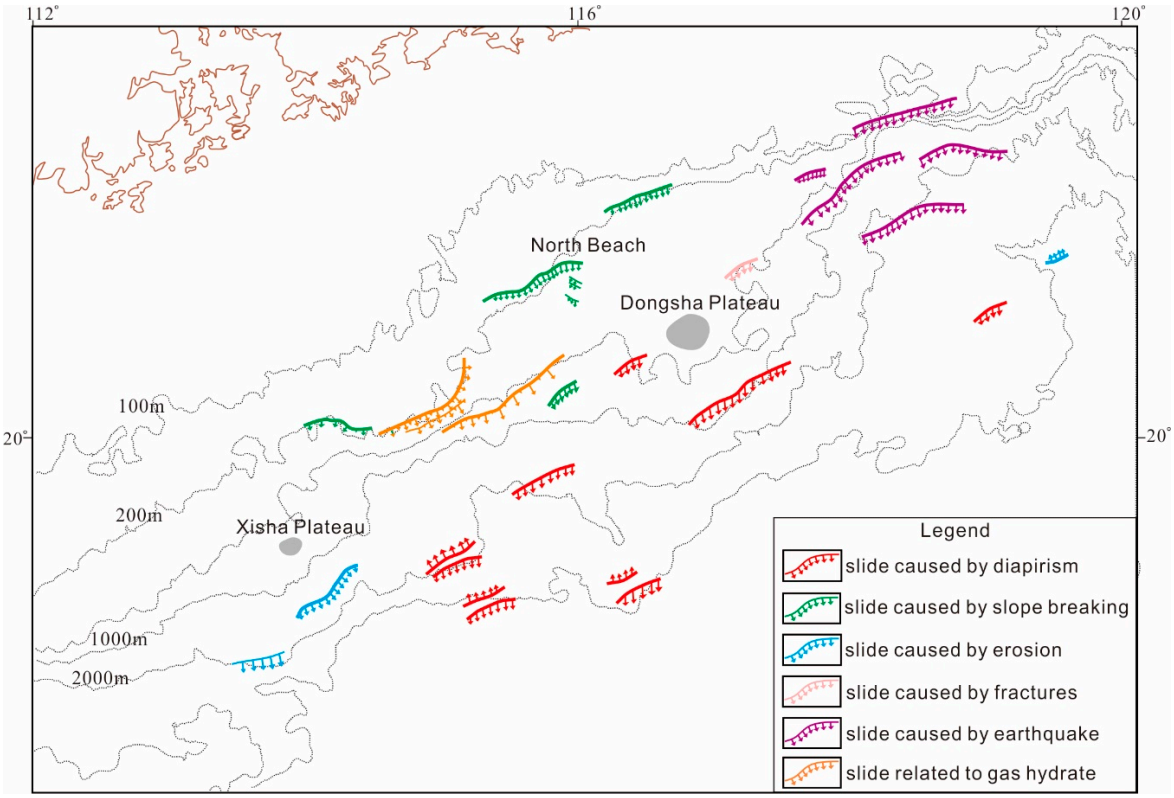

Figure 12. Distribution of different types of landslides in gas hydrate deposit area in the northern slope of South China Sea.

From the distribution of the different types of submarine landslides in the northern SCS (Figure 12), there are the following observations.

(1) Slope-break landslides (Figure 8) are found mainly along the slope of the northern SCS, and they are relatively large scale, display folds, and extend laterally towards the NE or ENE. The tectonic stresses were concentrated in the structural slope-break zone, where fractures and fissures are developed. Sediment loading also makes the strata unstable in this region, and this allows submarine landslides to form easily if there is any tectonic disturbance.

(2) The magmatism-related landslides (Figures 3 and 4) are located mainly on the deeper parts of the continental slope. Magmatic intrusions are common in the ocean–continent transition zone where there is an increase in water depth, a thinning of the continental crust, and the appearance of oceanic crust. Magmatic activity is strong in the southern part of Shenhu and in the Dongsha area. Magmatic diapers have cut across strata at depth, disturbed the overlying strata, and produced significant uplift in the form of arches, on the sides of which submarine landslides form [34].

(3) Erosion-related landslides (Figure 7) are typical of the Shenhu and Dongsha areas, where there are small-scale belts of erosion-related landslides. The landslides occur mainly along canyons or grooves formed by erosion. The complex terrain of canyon areas means that sediments on both sides of the valleys and their shoulders are prone to failure. In addition, the lithologies of sediments in buried rivers or valleys formed by erosion are usually different from those of the surrounding rocks, which makes these rocks prone to landslide [34,49].

(4) Fault-related landslides (Figure 5) are found mainly in the Dongsha area, and they are relatively small in scale. Their formation may be related to the large number of faults and neotectonic movements that have developed in the area since the late Miocene, thus inducing submarine landslides.

(5) Seismic-related landslides (Figure 6) are concentrated in the Dongsha area, and they have a clear relationship with the center of seismic activity in this area. As previously mentioned, the submarine landslides near where the epicenters are concentrated in the northeast of the Dongsha area are expected to be earthquake landslides.

(6) The hydrate-related landslides (Figures 9–11) are distributed mainly in the continental slope-break zone of the Shenhu area. Numerous studies have shown that the dissociation of gas hydrates in the late Quaternary led to submarine slumping and landslide formation worldwide [50], and examples are the Storegga submarine landslide off the coast of Norway and the Black Feather Landslide of Cape Fear off the coast of North Carolina [51]. Increasing evidence shows there to have been several periods of large-scale and rapid decomposition of gas hydrates on the northern slope of the South China Sea during the late Quaternary [42,52–55]. Therefore, the large amount of geological, geophysical, and geochemical data indicate that a large number of hydrate decomposition events took place in the study area. Hydrate decomposition can release large amounts of methane and water. When the fluids containing gas and water are transferred into the deposits, the shear strength of the sediments is decreased, and the sediments are de-stabilized, all of which can lead to the development of a typical large-scale submarine landslide.

6. Discussion

Gas hydrates and submarine landslides are always in a dynamic relationship. After an ancient seabed landslide has stabilized, the gas would move vertically along faults or gas chimneys or laterally along unconformity surfaces. Under the suitable temperature and pressure conditions, the stable initial state of the gas hydrate can be reached, thus BSR can be characterized in seismic profile. New tectonic movements may lead to gas hydrate decomposition and a new stage of landslides, and the new landslides will destroy the stable temperature and pressure conditions of the already-formed gas hydrates, causing hydrate decomposition. After the movement of these new landslides is complete, gas hydrates may develop again (Figures 9 and 11). Wu et al. [34] considered that the development of a submarine landslide is a retrogressive development, meaning that the landslides that initially form on the lower slopes subsequently exchange gas and water to perturb the upper sediments, thus forming a second generation of landslides. Such a process of repeated exchange of gas and water constitutes a mechanism for the repeated disturbance of the landslides, and the gradual moving backwards of the slope.

As shown in Table 1, The hydrate-related landslides have been divided further into pre-hydrate landslides, post-hydrate landslides, and syn-hydrate landslides.

Table 1. Classification of submarine landslides in the northern slope of SCS [34].

Criteria	Classification	Feature
Slip scale	Small landslides	Volume < 3×10^4 m^3
	Medium landslides	volume (3~50) $\times$ 10^4 m^3
	Large landslides	volume (50~300) $\times$ 10^4 m^3
	Very large landslides	Volume > 300×10^4 m^3
Slip body thickness	Thin landslides	Slip body thickness < 6 m
	Mid - level landslides	Slip body thickness < 6~20 m
	Thick landslides	Slip body thickness 20~50 m
	Very thick landslides	Slip body thickness > 50 m

Table 1. *Cont.*

Criteria	Classification		Feature
Structure of sliding slope and position of sliding surface	No layer landslides		Curved sliding surface in a uniform non-layered rock mass
	Along layer landslides		Slanting determined by slope structure
	Cutting layer landslides		Sliding surface intersects with strata of various constituents
Main factor	Magmatism landslide		Formation of magma caused by folds or skew resulted in landslides
	Fault related landslides		Fracture activity causes landslides to occur
	Seismicity related landslides		Earthquake caused landslides to occur
	Erosion-related landslides		Erosion caused strata instability
	Slope break landslides		Slope of slope-belt lead to inclination angle
	Hydrate-related landslides	Pre-hydrate landslides	Landslides occurred before hydrate formation
		syn-hydrate landslides	Landslides accurred during hydrates formed
		Post-hydrate landslides	Landslides occurred after hydrate formation

Buried landslides exist in the study area, and they are also called early landslides or ancient landslides. In the seismic profile (Figures 7, 8 and 11), mixed and disorderly deposits can be seen along a certain level below the seabed, buried by sediments. Locally, the overlying sediments represent normal deposition, without any evidence of landslide, but sometimes the upper coatings are new landslides, demonstrating the multi-stage nature of the landslide activity (Figures 4 and 9).

According to previous studies [8,49,56,57], the main factors affecting submarine landslides are as follows.

(1) Lithology. Submarine landslides occur mainly in loose sediments. Shallow sections, sediment samples, and geotechnical data show that the upper parts of landslides are made up of coarse- or fine-grained sands whereas the lower parts are clayey sands, with clay contents increasing downwards, sometimes with clay interlayers, shown in Figure 2.

(2) Terrain slope. As shown in Figure 7, The landslides tend to be initiated at the edge of the continental shelf where the slope steepens towards the open ocean, and where the forces of gravity can carry any de-stabilized sediment downslope. The landslides eventually stop when the slope becomes gentler or where there is a platform of some sort.

(3) Earthquakes, and waves. In Figure 6, we can see earthquakes directly damage sedimentary structures, reduce the cohesion of sediments on the seabed, and induce the initiation of a landslide, which will then continue moving under the force of gravity. Strong waves may also de-stabilize the sediments, leading to the production of a landslide.

(4) Gas hydrate decomposition. Natural gas hydrates are metastable materials that exist only in a narrow range of temperatures and pressures. An increase in temperature or a decrease in pressure is likely to cause the decomposition of the gas hydrate from a solid to a mixed state of gas and water, and the released gas can over-pressurize and destabilize the strata [49]. Meanwhile, any seismic activity or changes in the sediment load may result in these de-stabilized strata collapsing to produce a submarine landslide [34], as shown in Figure 11.

7. Conclusions

(1) According to the triggering factors for landslides, there are six major types of submarine landslide on the northern slope of the SCS, namely magmatism-related landslides,

fault-related landslides, seismicity-related landslides, erosion-related landslides, slope-break landslides, and hydrate-related landslides. The hydrate-related landslides can be divided further into pre-, post-, and syn-hydrate landslides. The seismic profiles of these kinds of landslide are shown from Figures 2–11.

(2) The landslides are located mainly on the continental slope, and on the flanks of volcanoes, valleys, and uplifted zones related to magma intrusions. We conclude the landslides extend laterally towards the NE or NEE (Figure 12), and their locations have close relationships with the ancient coastline and the steep seabed terrain.

(3) According to the seismic data acquired in Shenhu and Dongsha area. We conclude that the distribution and characteristics of the seabed landslides are closely related to the geological and tectonic settings, and the nature of the sedimentary deposits on the continental slope. The strata stability is related to the occurrence of both hydrates and magmatic sills, including sills and volcanic cones. Seismic activity is the important factor controlling the submarine landslide in Dongsha area, but the important factor controlling the submarine landslides in Shenhu area is the decomposition of natural gas hydrates.

Author Contributions: Conceptualization, Q.L. and Y.M.; methodology, X.W.; validation, Z.X., L.L. and M.H.; formal analysis, Y.H.; writing—original draft preparation, X.W.; writing—review and editing, X.W. and Q.L.

Funding: This research was funded by the National Special Project on Gas Hydrate of China grant number GZH201100301, GZH201100311, DD20160217, and Special Funding from Yangtze Normal University grant number 2017KYQD71.

Acknowledgments: We thank crews of Tanbao vessel for collecting the 2D seismic data used in this study. The authors are grateful to S.Z. Li (Ocean University of China) for tectonic geology distinguish of the study area. We also acknowledge Prof. D. Feng and the two anonymous reviewers for their helpful comments and suggestions. This study was financially supported by National Special Project on Gas Hydrate of China (Grant: GZH201100301, GZH201100311, DD20160217) and Special Funding from Yangtze Normal University (Grant: 2017KYQD71).

Conflicts of Interest: The authors declare no conflict of interest

References

1. Mulder, T.; Cochonat, P. Classification of offshore mass movements. *J. Sediment. Res.* **1996**, *66*, 43–57.
2. Baum, R.L.; Savage, W.Z.; Wasowski, J. Mechanics of earthflows. In Proceedings of the International Workshop on Occurrence and Mechanisms of Flow-Like Landslides in Natural Slopes and Earthfills, Bologna, Italy, 14–16 May 2003; pp. 185–190.
3. Solheim, A.; Berg, K.; Forsberg, C.F.; Bryn, P. The Storegga Slide complex: Repetitive large scale sliding with similar cause and development. *Mari. Pet. Geol.* **2005**, *22*, 97–107. [CrossRef]
4. Mountjoy, J.J.; McKean, J.; Barnes, P.M.; Pettinga, J.R. Terrestrial-style slow-moving earthflow kinematics in a submarine landslide complex. *Mar. Geol.* **2009**, *267*, 114–127. [CrossRef]
5. Wech, A.G.; Creager, K.C. A continuum of stress, strength and slip in the Cascadia subduction zone. *Nat.Geosci.* **2011**, *4*, 624–628. [CrossRef]
6. Hampton, M.A.; Lee, H.J.; Locat, J. Submarine landslides. *Rev. Geophys.* **1996**, *34*, 33–59. [CrossRef]
7. Song, H. Researches on dynamic evolution of gas hydrate system (II): Submarine slides. *Prog. Geophys.* **2003**, *18*, 503–511.
8. Brown, H.E.; Holbrook, W.S.; Hornbach, M.J.; Nealon, J. Slide structure and role of gas hydrate at the northern boundary of the Storegga Slide, offshore Norway. *Mar. Geol.* **2006**, *229*, 179–186. [CrossRef]
9. Haeussler, P.; Lee, H.; Ryan, H.; Labay, K.; Suleimani, E.; Alexander, C.; Kayan, R. Submarine landslides and tsunamis at Seward and Valdez triggered by the 1964 magnitude 9.2 Alaska earthquake. *Newsl. Alsk. Geol.* **2008**, *39*, 1–2.
10. Kawamura, K.; Laberg, J.S.; Kanamatsu, T. Potential tsunamigenic submarine landslides in active margins. *Mar. Geol.* **2014**, *356*, 44–49. [CrossRef]
11. Barnes, P.M.; Pecher, I.; LeVay, L. Expedition 372 Scientific Prospectus: Creeping Gas Hydrate Slides and LWD for Hikurangi Subduction Margin. *Int. Ocean Discov. Program* **2017**. [CrossRef]

12. Makogon, Y.F.; Holditch, S.A.; Makogon, T.Y. Natural gas-hydrates—A potential energy source for the 21st century. *J. Pet. Sci. Eng.* **2007**, *56*, 14–31. [CrossRef]
13. Cristián, R.; Vera, E.; Antonio, G. Seismic analysis and distribution of a bottom-simulating reflector (BSR) in the chilean margin offshore of valdivia (40° s). *J. South Am. Earth Sci.* **2009**, *27*, 1–10.
14. Micallef, A.; Masson, D.G.; Berndt, C.; Stow, D.A.V. Development and mass movement processes of the north-eastern storegga slide. *Quat. Sci. Rev.* **2009**, *28*, 433–448. [CrossRef]
15. Urlaub, M.; Talling, P.J.; Masson, D.G. Timing and frequency of large submarine landslides: Implications for understanding triggers and future geohazard. *Quat. Sci. Rev.* **2013**, *72*, 63–82. [CrossRef]
16. Smith, D.E.; Harrison, S.; Jordan, J.T. Sea level rise and submarine mass failures on open continental margins, 2013. *Quat. Sci. Rev.* **2013**, *82*, 93–103. [CrossRef]
17. Zander, T.; Choi, J.C.; Vanneste, M.; Berndt, C.; Dannowski, A.; Carlton, B.; Bialas, J. Potential impacts of gas hydrate exploitation on slope stability in the Danube deep-sea fan, black sea. *Mar. Pet. Geol.* **2017**, *92*, 1056–1068. [CrossRef]
18. Crutchley, G.J.; Geiger, S.; Pecher, I.A.; Gorman, A.R.; Zhu, H.; Henrys, S.A. The potential influence of shallow gas and gas hydrates on sea floor erosion of Rock Garden, an uplifted ridge offshore of New Zealand. *Geo-Mar. Lett.* **2010**, *30*, 283–303. [CrossRef]
19. Phrampus, B.J.; Hornbach, M.J. Recent changes to the Gulf Stream causing widespread gas hydrate dissociation. *Nature* **2012**, *490*, 527–530. [CrossRef] [PubMed]
20. Mountjoy, J.J.; Krastel, S.; Gross, F.; Pecher, I. Large creepy landslides controlled by gas hydrates? Rheological control or cyclic gas flux from the base of hydrate stability. In Proceedings of the Gordon Research Conference, Galveston, TX, USA, 28 February–4 March 2016.
21. Borrell, N.; Somoza, L.; León, R.; Medialdea, T.; Gonzalez, F.J.; Gimenezmoreno, C.J. GIS Catalogue of Submarine Landslides in the Spanish Continental Shelf: Potential and Difficulties for Susceptibility Assessment. 2016. Available online: https://link.springer.com/chapter/10.1007%2F978-3-319-20979-1_50 (accessed on 4 November 2018).
22. Somoza, L.; Medialdea, T.; Gonzalez, F.J. *Giant Mass-Transport Deposits in the Southern Scotia Sea (Antarctica)*; Geological Society: London, UK, 2018; Volume 477.
23. Yelisetti, S. Seismic Structure, Gas Hydrate, and Slumping Studies on the Northern Cascadia Margin Using Multiple Migration and Full Waveform Inversion of OBS and MCS Data. Ph.D. Thesis, University of Victoria, Victoria, BC, Canada, 2014.
24. Yelisetti, S.; Spence, G.D.; Riedel, M. Role of gas hydrates in slope failure on frontal ridge of northern Cascadia margin. *Geophys. J. Int.* **2014**, *199*, 441–458. [CrossRef]
25. Zhang, H.Q.; Yang, S.X.; Wu, N.Y.; Schultheiss, P. China's first gas hydrate expedition successful. *Fire in the Ice: Methane Hydrate Newsl.* **2007**, *7*, 4–8.
26. Zhang, G.X.; Yang, S.X.; Zhang, M.; Liang, J.Q.; Lu, J.A.; Holland, M.; Schultheiss, P.; the GMGS2 Science Team. GMGS2 expedition investigates rich and complex gas hydrate environment in the South China Sea. *Fire Ice Methane Hydrate Newsl.* **2014**, *14*, 1–5.
27. Yang, S.X.; Zhang, M.; Liang, J.Q.; Lu, J.A.; Zhang, Z.J.; Holland, M.; Schultheiss, P.; Fu, S.Y.; Sha, Z.B.; the GMGS3 Science Team. Preliminary results of China's third gas hydrate drilling expedition: A critical step from discovery to development in the South China Sea. *Fire Ice Methane Hydrate Newsl.* **2015**, *15*, 1–5.
28. Sha, Z.B.; Liang, J.Q.; Zhang, G.X.; Yang, S.X.; Lu, J.A.; Zhang, Z.J.; McConnell, D.R.; Humphrey, G. A seepage gas hydrate system in northern South China Sea: Seismic and well log interpretations. *Mar. Geol.* **2015**, *366*, 69–78. [CrossRef]
29. Feng, Z.Q.; Feng, W.K.; Xue, W.J.; Liu, Z.; Chen, J.; Li, W. *Evaluation of Marine Geologic Hazards and Engineering Geological Conditions in the Northern South China Sea*; Hehai University Publish: Nanjing, China, 1996.
30. Xia, Z.; Zheng, T.; Pang, G.C. Features of submarine geological hazards in northern South China Sea. *Trop. Oceanol.* **1999**, *18*, 91–95.
31. Liu, S.Q.; Liu, X.Q.; Wang, S.J.; Guo, Y.G. Discussion on Some Problems in Compilation of Hazardous Geological Map (1:2,000,000) of South China Sea. *Chin. J. Geol. Hazard Control.* **2002**, *13*, 17–20.
32. Li, Z.W. Research on Hazardous Geological Factors in the Outer Shelf of Northern South China Sea and Influence on the Submarine Pipelines. Ph.D. Thesis, Institute of Oceanology, Chinese Academy of Science, Qingdao, China, 2011.

33. Zhou, C.; Fan, F.X.; Luan, Z.D.; Ma, X.C.; Yan, J. Geomorphology and hazardous geological factors on the continental shelf of the northern South China Sea. *Mar. Geol. Front.* **2013**, *29*, 51–60.
34. Ma, Y.; Li, S.Z.; Xia, Z.; Zhang, B.; Wang, X.; Cheng, S. Characteristics of Hazardous Geological Factors on Shenhu Continental Slope in the Northern South China Sea. *Earth Sci.* **2014**, *39*, 1364–1372.
35. Zhu, C.Q.; Jia, Y.G.; Liu, X.L.; Zhang, H.; Wen, Z.M.; Huang, M.; Shan, H.X. Classification and genetic mechanism of submarine landslide: A review. *Mar. Geol. Quat. Geol.* **2015**, *35*, 153–163.
36. Feng, W.K.; Shi, Y.H.; Chen, L.H. Research for seafloor landslide stability on the outer continental shelf and the upper continental slope in the northern South China Sea. *Mar. Geol. Quat. Geol.* **1994**, *14*, 81–94.
37. Sun, Y.B.; Wu, S.G.; Wang, Z.J.; Li, Q.P.; Wang, X.J.; Dong, D.D.; Liu, F. The geometry and deformation characteristics of Baiyun submarine landslide. *Mar. Geol. Quat. Geol.* **2008**, *28*, 69–77.
38. Wu, S.G.; Chen, S.S.; Wang, Z.J.; Li, Q.P. Submarine landslide and risk evaluation on its instability in the deepwater continental margin. *Geoscience* **2008**, *22*, 430–437.
39. Liu, F. Submarine Landslides and Its Environmental Risk Assessment by Gas Hydrate Decomposition in the Northern Slope of the South China Sea. Ph.D. Thesis, Graduate University of Chinese Academy of Sciences, Beijing, China, 2010.
40. Liu, F.; Wu, S.G.; Sun, Y.B. A quantitative analysis for submarine slope instability of the northern South China Sea due to gas hydrate dissociation. *Chin. J. Geophys.* **2010**, *53*, 946–953.
41. Wu, S.G.; Qin, Z.L.; Wang, D.W.; Peng, X.C.; Wang, Z.J.; Yao, G.S. Seismic characteristics and triggering mechanism analysis of mass transport deposits in the northern continental slope of the South China Sea. *Chin. J. Geophys.* **2011**, *54*, 3184–3195. [CrossRef]
42. Chen, H.J.; Huang, L.; Peng, X.C.; Wu, J.Q.; Li, W.C. Discussion of characteristics and formation of landslide zones in the gas hydrate survey area of northwest continental slope, the South China Sea. *J. Trop. Oceanogr.* **2012**, *51*, 4137–4140.
43. Li, J.F.; Ye, J.L.; Qin, X.W.; Qiu, H.J.; Wu, N.Y.; Lu, H.L.; Xie, W.W.; Lu, J.A.; Peng, F.; Xu, Z.Q.; et al. The first offshore natural gas hydrate production test in South China Sea. *China Geol.* **2018**, *1*, 5–16. [CrossRef]
44. Ye, J.L.; Qin, X.W.; Qiu, H.J.; Liang, Q.Y.; Dong, Y.F.; Wei, J.G.; Lu, H.L.; Lu, J.A.; Shi, Y.H.; Zhong, C.; et al. Preliminary results of environmental monitoring of the natural gas hydrate production test in the South China Sea. *China Geol.* **2018**, *1*, 202–209. [CrossRef]
45. Wang, X.F.; Li, S.Z.; Gong, Y.H.; Xin, L.; Suo, Y.H.; Dai, L.M.; Yun, M.; Zhang, B.K. Active Tectonics and Its Effects on Gas-Hydrates in Northern South China Sea. *J. Jilin Univ.* **2014**, *44*, 419–431.
46. Li, S.Z.; Suo, Y.H.; Liu, X.; Dai, L.M.; Yu, S.; Zhao, S.J.; Ma, Y.; Wang, X.F.; Cheng, S.X.; An, H.T.; et al. Basin dinamics and basin groups of the South China Sea. *Mar. Geol. Quat. Geol.* **2012**, *32*, 55–78. [CrossRef]
47. Wan, L.; Yao, B.C.; Wu, N.Y.; Ma, K.Y.; Dong, Y.J. Cenozoic geological characteristics in the west of the South China Sea. *Mar. Geol. Quat. Geol.* **2005**, *25*, 45–52.
48. He, J.; Liang, Q.Y.; Ma, Y.; Shi, Y.H.; Xia, Z. Geohazards types and their distribution characteristics in the natural gas hydrate area on the northern slope of the South China Sea. *Geol. China* **2018**, *45*, 15–28.
49. Ma, Y. Study of Submarine Landslides and Trigger Mechanism along the Continental Slope of the Northern South China Sea. Ph.D. Thesis, Ocean University of China, Qingdao, China, 2014.
50. Wild, J.J. Seismic velocities beneath creeping gas hydrates slides: Analysis of ocean bottom seismometer data in the Tuaheni Landslide Complex on the Hikurangi margin, New Zealand. Master's Thesis, University of Auckland, Auckland, New Zealand, 2016.
51. Rodriguez, N.M.; Paull, C.K. Data Report: 14C Dating of Sediment of the Uppermost Cape Fear Slide Plain: Constraints on the Timing of This Massive Submarine Landslide. In Proceedings of the Ocean Drilling Program, Galveston, Tx, USA, 2000; Volume 164, pp. 325–327.
52. Lu, M.A.; Ma, Z.J.; Chen, M.H.; Sui, S.Z. The δ13C fast negative event and its cause during the penultimate deglacial stage of West Pacific Marginal Sea. *Quat. Sci.* **2002**, *38*, 349–358.
53. Ye, L.M.; Chu, F.Y.; Ge, Q.; Xu, D. A Rapid gas hydrate dissociation in the Northern South China Sea since the Late Younger Dryas. *Earth Sci. J. China Univ. Geosci.* **2013**, *38*, 1299–1308.
54. Chen, F.; Zhou, Y.; Zhuang, C.; Lu, H.F.; Wu, C. Origin of the hiatus of last glacial period in cold seep area of northeastern South China Sea. *Mar. Geol. Quat. Geol.* **2016**, *36*, 19–27.
55. Zhuang, C.; Chen, F.; Cheng, S.H.; Lu, H.F.; Wu, C.; Cao, J.; Duan, X. Light carbon isotope events of foraminifera attributed to methane release from gas hydrates on the continental slope, northeastern South China Sea. *Sci. China Earth Sci.* **2016**, *59*, 1981–1995. [CrossRef]

56. Sun, Y.B. The Mechanism and Prediction of Deepwater Geohazard in the Northern of South Sea. Ph.D. Thesis, Institute of Oceanology, Chinese Academy of Science, Qingdao, China, 2011.
57. Wei, L. Seismic Characteristics and Trigger Mechanisms of Submarine Landslides in Northern South China Sea. Ph.D. Thesis, Institute of Oceanology, Chinese Academy of Science, Qingdao, China, 2013.